

# Anomalous diffusion and the structure of human transportation networks

D. Brockmann<sup>a</sup>

Max-Planck-Institute for Dynamics and Self-Organization

**Abstract.** The dispersal of individuals of a species is the key driving force of various spatiotemporal phenomena which occur on geographical scales. It can synchronise populations of interacting species, stabilise them, and diversify gene pools [1–3]. The geographic spread of human infectious diseases such as influenza, measles and the recent severe acute respiratory syndrome (SARS) is essentially promoted by human travel which occurs on many length scales and is sustained by a variety of means of transportation [4–8]. In the light of increasing international trade, intensified human traffic, and an imminent influenza A pandemic the knowledge of dynamical and statistical properties of human dispersal is of fundamental importance and acute [7,9,10]. A quantitative statistical theory for human travel and concomitant reliable forecasts would substantially improve and extend existing prevention strategies. Despite its crucial role, a quantitative assessment of human dispersal remains elusive and the opinion that humans disperse diffusively still prevails in many models [11]. In this chapter I will report on a recently developed technique which permits a solid and quantitative assessment of human dispersal on geographical scales [12]. The key idea is to infer the statistical properties of human travel by analysing the geographic circulation of individual bank notes for which comprehensive datasets are collected at the online bill-tracking website [www.wheresgeorge.com](http://www.wheresgeorge.com). The analysis shows that the distribution of travelling distances decays as a power law, indicating that the movement of bank notes is reminiscent of superdiffusive, scale free random walks known as Lévy flights [13]. Secondly, the probability of remaining in a small, spatially confined region for a time  $T$  is dominated by heavy tails which attenuate superdiffusive dispersal. I will show that the dispersal of bank notes can be described on many spatiotemporal scales by a two parameter continuous time random walk (CTRW) model to a surprising accuracy. To this end, I will provide a brief introduction to continuous time random walk theory [14] and will show that human dispersal is an ambivalent, effectively superdiffusive process.

## 1 Dispersal ecology

The notion of dispersal in ecology usually refers to the movement of individuals of a species in their natural environment [1,3]. The statistical properties of dispersal can be quantified by the dispersal curve  $p_{\Delta t}(\Delta \mathbf{x})$ . The dispersal curve reflects the relative frequency of geographic displacements  $\Delta \mathbf{x}$  which are traversed within a given period of time  $\Delta t$ . In the ecological literature, the term “dispersal” is commonly used in the context of the spatial displacement of individuals of a species between their geographical origin of birth and the location of their first breeding place, a process which occurs on time scales of the lifespan of the individuals. Here we make use of the notion of dispersal somewhat differently, referring to geographical displacements

---

<sup>a</sup> e-mail: [brockmann@ds.mpg.de](mailto:brockmann@ds.mpg.de)

that occur on much shorter timescales of the order of days. A large class of dispersal curves (for example, exponential, gaussian, stretched exponential) exhibit a characteristic length scale [15]. That is, when interpreted as the probability of finding a displacement of length  $\Delta\mathbf{x}$ , a length scale can be defined by the square root of second moment, i.e.  $\sigma = \sqrt{\langle \Delta\mathbf{x}^2 \rangle}$ . The existence of a typical length scale often justifies the description of dispersal in terms of diffusion equations on spatiotemporal scales larger than  $\Delta t$  and  $\sigma$  [16]. Because, if single displacements are sufficiently uncorrelated the probability density  $W(\mathbf{x}, t)$  of having traversed a total displacement  $\mathbf{X}(t)$  after time  $t$  is a Gaussian which obeys Fick's second law:

$$\partial_t W = D \partial_x^2 W, \quad (1)$$

where  $D = \sigma^2/\Delta t$  is the diffusion coefficient. This result is a consequence of the central limit theorem [17] and does not depend on the precise form of the short time dispersal curve as long as the variance  $\langle \Delta x^2 \rangle$  is finite.

## 2 Diffusive dispersal and reaction kinetics

In population dynamical systems this type of diffusive dispersal is quite frequently combined with a reaction kinetic scheme which accounts for local interactions between various types of reacting agents, for example various species in predator-prey systems. Sometimes groups of individuals of a single species which interact are classified according to some criterion. For instance in the context of epidemiology a population is often classified according to their infective status.

In an approximation which neglects the intrinsic fluctuations of the underlying reaction kinetics one obtains for these systems mean field reaction-diffusion equations, the most prominent example of which is the Fisher equation<sup>1</sup> [18],

$$\partial_t u = \lambda u(1 - u) + D \partial_x^2 u, \quad (2)$$

for the concentration  $u(\mathbf{x}, t)$  of a certain class of individuals, a species etc.

### 2.1 SIS dynamics

A paradigmatic system which naturally yields a description in terms of Eq. (2) and which has been used to describe the geographic spread of infectious diseases is the SIS-model in which a local population of  $N$  individuals segregates into the two classes of a) susceptibles  $S$  who may catch a disease and b) infecteds  $I$  who transmit it. Transmission is quantified by the rate  $\alpha$  and recovery by the rate  $\beta$  [11]. The reaction scheme could not be simpler:



In the limit of large population size  $N$  the dynamics can be approximated by the set of differential equations

$$\partial_t S = -\alpha IS/N, \quad \partial_t I = \alpha IS/N - \beta I. \quad (4)$$

Assuming that the number of individuals is conserved (i.e.  $I(t) + S(t) = N$ ) and that disease transmission is more frequent than recovery ( $\alpha > \beta$ ) one obtains for the rescaled relative number of infecteds  $u(t) = \alpha I(t)/N(\alpha - \beta)$  a single ordinary differential equation (ODE):

$$\partial_t u = \lambda u(1 - u), \quad (5)$$

where  $\lambda = \alpha - \beta$ . If, additionally reactants are free to move diffusively one obtains Eq. (2) for the dynamics of the relative number of infecteds  $u(\mathbf{x}, t)$  as a function of position and time.

<sup>1</sup> Also referred to as the Fisher-Kolmogorov-Petrovsky-Piscounov equation.

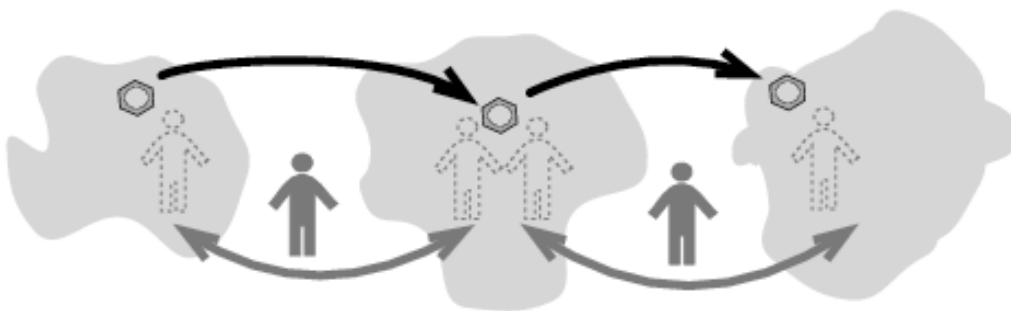


**Fig. 1.** Human travel and the dispersal of pathogens. The gray areas depict home ranges of individuals. By virtue of overlapping home ranges and inter-homerange travel an infectious disease spreads in space. Although humans travel back and forth between home ranges, pathogens spread continuously in space.

## 2.2 A word of caution

The popularity and success of the Fisher-equation and similar equations in the field of theoretical biology can be ascribed to some extent to the fact that they possess propagating front solutions and that qualitatively similar patterns were observed in historic pandemics, the most prominent example of which is the bubonic plague pandemic of the 14th century which crossed the European continent as a wave within three years at an approximate speed of a few kilometers per day. Aside from factors which are known to play a role, such as social contact networks, age structure, inhomogeneities in local populations and inhomogeneities in the geographic distribution of the population, there is something fundamentally wrong with the diffusion assumption on which this class of equations is based upon. Humans (with the exception maybe of nomads) do not and never did diffuse on timescales much shorter than their lifespan. A simple argument can be given why this cannot be so. For a diffusion process the expected time for returning to the point of origin is infinite [19] (despite the fact that in spatial dimensions  $d \leq 2$  the probability of returning is unity). It would not make much sense to have a home if the expected time to return to it is infinite. However, in the context of the geographic spread of infectious diseases it does at times make sense to employ reaction-diffusion equations. That is because the position of what is passed from human to human, i.e. the pathogens, is what matters and not the position of single host individuals. Unlike humans, pathogens are passed from human to human and opposed to humans pathogens have no inclination of returning. They disperse diffusively and a description in terms of reaction-diffusion dynamics is justified, see Fig. 1.

## 3 Long distance dispersal and Lévy flights

Recently the notion of long distance dispersal (LDD) has been established in dispersal ecology [20], taking into account the observations that a number of dispersal curves exhibit long, algebraic tails which forbid the identification of a typical scale and thus a description of dispersal phenomena based on diffusion equations. If, for instance, the probability density of traversing a distance  $r$  in a given period of time  $\Delta t$  decreases according to

$$p_{\Delta t}(r) \sim \frac{1}{r^{1+\beta}} \quad (6)$$

with a tail exponent  $\beta < 2$ , the variance of the displacement magnitude is infinite and consequently no typical length scale can be identified. Power-law distributions are abundant in nature. Meteorite sizes, city sizes, income and the number of species per genus follow power-law distributions [21]. In the context of animal movements such power-laws have been observed in foraging movements of an increasing number of species, bumble bees and deer [22], microzooplankton [23], reindeer [24], albatrosses [25], spider monkeys [26] and jakaals [27], to name a few.

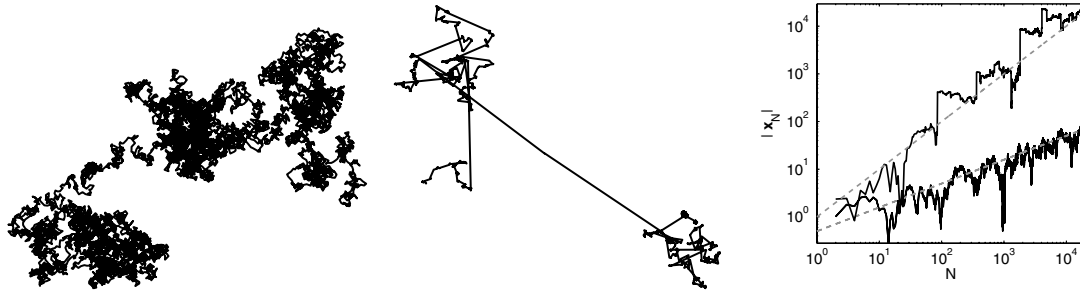


**Fig. 2.** Ordinary random walks and Lévy flights. Left: the trajectory of an ordinary random walk in two dimensions, equivalent to Brownian motion on large spatiotemporal scales. Middle: unlike Brownian motion, the trajectory of the two-dimensional Cauchy-process, i.e. a Lévy flight with Lévy exponent  $\beta = 1$  exhibits local clustering interspersed with long distance jumps. Right: the distance  $|\mathbf{X}_N|$  from the starting point  $\mathbf{X}_0 = 0$  of an ordinary random walk (lower trajectory) and a Lévy flight ( $\beta = 1$ , upper trajectory) as a function of step number  $N$ . The dashed lines indicate the scaling  $N^{1/2}$  and  $N^{1/\beta}$  respectively. Clearly, the Lévy flight is superdiffusive.

### 3.1 Lévy flights

In physics, random walk processes with a power-law single-step distribution are known as Lévy flights [14, 28–30]. Due to the lack of scale in the single steps, Lévy flights are qualitatively different from ordinary random walks. Unlike ordinary random walks the position  $\mathbf{X}_N = \sum_n^N \Delta \mathbf{x}_n$  after  $N$  steps  $\Delta \mathbf{x}_n$  scales with the number of steps according to

$$\mathbf{X}_N \sim N^{1/\beta} \quad (7)$$

with  $\beta < 2$ . Thus, Lévy flights disperse “faster” than the ordinary  $N^{1/2}$  behavior exhibited by ordinary random walks; Lévy flights are superdiffusive. Furthermore, the probability density for the position  $p(\mathbf{x}, N)$  for Lévy flights behaves asymptotically as

$$p(\mathbf{x}, N) \sim N^{-D/\beta} L_\beta \left( \mathbf{x}/N^{1/\beta} \right) \quad (8)$$

where  $D$  is the spatial dimension and the function  $L_\beta$  is known as the symmetric Lévy-stable law of index  $\beta$ . This limiting function is a generalization of the ordinary Gaussian and can be expressed by its Fourier-transform

$$L_\beta(\mathbf{z}) = \frac{1}{(2\pi)^{D/2}} \int d\mathbf{k} e^{-i\mathbf{z} \cdot \mathbf{k}} \exp(-|\mathbf{k}|^\beta). \quad (9)$$

The limiting value  $\beta = 2$  corresponds to the Gaussian, the limiting function for ordinary random walks. The lack of scale in a Lévy flight, its superdiffusive nature and the geometrical difference between Lévy flights and ordinary random walks are illustrated in figure 2. Lévy flights, and superdiffusive random motion was observed in a variety of physical and biological systems, ranging from transport in chaotic systems [31] to foraging patterns of wandering albatrosses [25] and spider monkeys [26].

## 4 Human travel in the 21st century

Nowadays, humans travel on many spatial scales, ranging from a few to thousands of kilometres over short periods of time. A person in the 21st century can reach virtually any point on the globe in a matter of days. The intensity of modern human travel is convincingly illustrated in Fig. 3 which depicts nearly the entire international air traffic network.



**Fig. 3.** Worldwide air traffic network. Links represent routes between the 500 most frequented airports. Brightness indicates the intensity of traffic between nodes.

The direct quantitative assessment of human movements, however, is difficult, and a statistically reliable estimate of human dispersal comprising all spatial scales does not exist. Contemporary models for the spread of infectious diseases across large geographical regions have to make assumptions on human travel. The notion that humans travel short distances more frequently than long ones is typically taken into account. Yet, the precise ratio of the frequency of short trips and the frequency of long trips is not known and must be assumed. Furthermore, it is generally agreed upon that human travel, being a complex phenomenon, adheres to complex mathematical rules with a lot of detail.

Recently, it was shown that the global spread of SARS in 2003 can be reproduced by a model which takes into account nearly the entire civil aviation network [7, 10]. Despite the high degree of complexity of aviation traffic, the strong heterogeneity of the network yields an unexpectedly narrow range of fluctuations, supporting the idea that reliable forecasts of the geographic spread of disease is possible. Although the model successfully accounts for the geographic spread on global scales, it cannot account for the spread on small and intermediate spatial scales. To this end a comprehensive knowledge of human travel on scales ranging from a few to a few thousand kilometers is necessary. However, collecting comprehensive traffic data for all means of human transportation involved is difficult if not impossible.

## 5 Money as a proxy for human travel

In a recent study [12, 32], the problem of measuring human travel directly was resolved by trick. Instead of measuring individual human travel paths directly, the geographic dispersal of bank notes in the United States was investigated instead. The key idea of the project was to use bank note dispersal as a proxy for human travel on all geographical length scales. The data was collected from the online bill-tracking website [www.wheresgeorge.com](http://www.wheresgeorge.com). The idea of this internet game, which was initiated in 1998 by Hank Eskin, is simple. Individual bank notes are marked by registered users and brought into circulation. When people come into possession of such marked bank notes, they can register at the website and report their current location and return the bank note into circulation. Thus, registered users can monitor the geographical dispersal of their money. Meanwhile, over 80 millions dollar bills have been registered and over 3 million users participate in the game. As bank notes are primarily transported by travelling

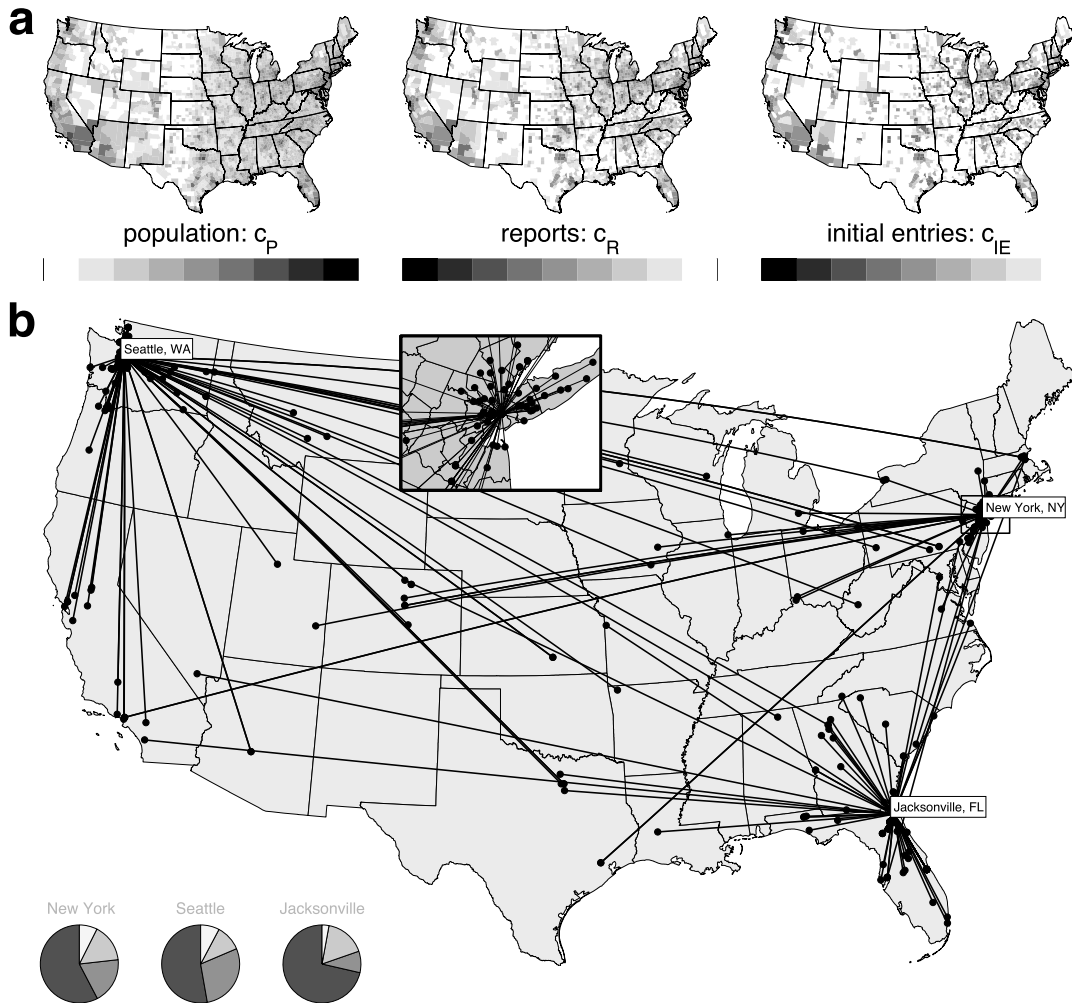


**Fig. 4.** Dispersal of bank notes on geographical scales. a) Relative logarithmic densities of population ( $c_P = \log_{10} \rho_P / \langle \rho_P \rangle$ ), reports ( $c_R = \log_{10} \rho_R / \langle \rho_R \rangle$ ) and initial entry ( $c_{IE} = \log_{10} \rho_{IE} / \langle \rho_{IE} \rangle$ ) as functions of geographical coordinates. The shades of gray encode the densities relative to the nation-wide averages (3,109 counties) of  $\langle \rho_P \rangle = 95.15$ ,  $\langle \rho_R \rangle = 0.34$  and  $\langle \rho_{IE} \rangle = 0.15$  individuals, reports and initial entries per  $\text{km}^2$ , respectively. b) Short time trajectories of bank notes originating from three different places. Tags indicate initial, symbols secondary report locations. Lines represent short time trajectories with travelling time  $T < 14$  days. The inset depicts a close-up of the New York area. Pie charts indicate the relative number of secondary reports coarsely sorted by distance. The fractions of secondary reports that occurred at the initial entry location (dark), at short ( $0 < r < 50$  km), intermediate ( $50 < r < 800$  km) and long ( $r > 800$  km) distances are ordered by increasing brightness. The total number of initial entries are  $N = 524$  (Seattle),  $N = 231$  (New York),  $N = 381$  (Jacksonville).

humans, the statistical properties of human travel can be inferred from the dispersal of bank notes with high spatio-temporal precision.

The original study of human movements was based on the trajectories of a subset of 464,670 dollar bills obtained from the website and the dispersal of bank notes in the United States, excluding Alaska and Hawaii, was analysed. The core data consisted of 1,033,095 reports to the website. From these reports the geographical displacements  $r = |\mathbf{x}_2 - \mathbf{x}_1|$  between a first ( $\mathbf{x}_1$ ) and secondary ( $\mathbf{x}_2$ ) report location of a bank note and the elapsed time  $T$  between successive reports was computed. The pairs of datapoints  $\{r_i, T_i\}$  represented the core dataset, from which

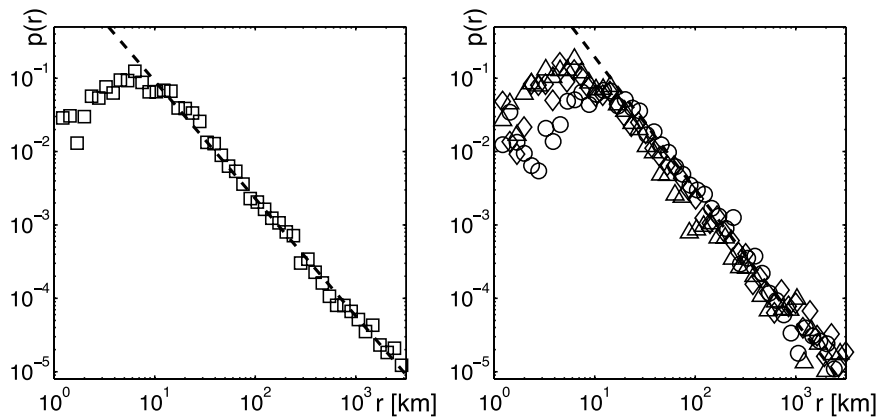


**Fig. 5.** Quantitative analysis of bank note dispersal. Left: the short time dispersal kernel. The measured probability density function  $p(r)$  of traversing a distance  $r$  in less than  $T = 4$  days is depicted by squares. It is computed from an ensemble of 20,540 short time displacements. The dashed black line indicates a power law  $p(r) \sim r^{-(1+\beta)}$  with an exponent of  $\beta = 0.59$ . Right:  $p(r)$  for three classes of initial entry locations (black triangles for metropolitan areas, diamonds for cities of intermediate size, and circles for small towns).

the probability density function (pdf)  $W(r, t)$  of having traveled a distance  $r$  after a time  $t$  was estimated.

In order to illustrate qualitative features of bank note trajectories, Fig. 4 depicts short time trajectories ( $T < 14$  days) originating from three major cities (Seattle, WA, New York, NY, Jacksonville, FL). Succeeding their initial entry, the majority of bank notes are reported next in the vicinity of the initial entry location, i.e.  $r < 10$  km (Seattle: 52.7%, New York: 57.7% Jacksonville: 71.4%). However, a small yet considerable fraction is reported beyond a distance of 800 km (Seattle: 7.8%, New York: 7.4%, Jacksonville: 2.9%).

### 5.1 The lack of scale in money movements

From a total of  $N = 20,540$  short time displacements one can measure the probability density  $p(r)$  of traversing a distance  $r$  in a time interval  $\delta T$  between one and four days. The result is depicted in Fig. 5. A total of 14,730 (i.e. a fraction  $Q = 0.71$ ) secondary reports occur outside a short range radius  $L_{\min} = 10$  km. Between  $L_{\min}$  and the approximate average east-west extension of the United States  $L_{\max} \approx 3,200$  km  $p(r)$  exhibits power law behaviour  $p(r) \sim r^{-(1+\beta)}$  with an exponent  $\beta = 0.59 \pm 0.02$ . For  $r < L_{\min}$ ,  $p(r)$  increases linearly with  $r$  which implies that displacements are distributed uniformly inside the disk  $|\mathbf{x}_2 - \mathbf{x}_1| < L_{\min}$ .

One might speculate whether the observed lack of scale in  $p(r)$  is not a dynamic property of dispersal but rather imposed by the substantial spatial inhomogeneity of the United States. For instance, the probability of traveling a distance  $r$  might depend strongly on static properties such as the local population density. In order to test this hypothesis,  $p(r)$  was measured for three classes of initial entry locations: highly populated metropolitan areas (191 locations, local population  $N_{\text{loc}} > 120,000$ ), cities of intermediate size (1,544 locations, local population  $120,000 > N_{\text{loc}} > 22,000$ ), and small towns (23,640 locations, local population  $N_{\text{loc}} < 22,000$ ) comprising 35.7%, 29.1% and 25.2% of the entire population of the United States, respectively. Fig. 5 also depicts  $p(r)$  for these classes. Despite systematic deviations for short distances, all distributions exhibit an algebraic tail with the same exponent  $\beta \approx 0.6$ . This confirms that the observed power-law is an intrinsic and universal property of dispersal, the first experimental evidence that bank note trajectories are reminiscent of Lévy flights and that their geographic dispersal is superdiffusive.

## 6 Is that all?

However, the situation is more complex. If one assumes that the dispersal of bank notes can be described by a Lévy flight with a short time probability distribution  $p(r)$  as depicted in Fig. 5, one can estimate the time  $T_{\text{eq}}$  for an initially localised ensemble of bank notes to reach the stationary distribution (maps in Fig. 4). Assume that the Lévy flight evolves in a two-dimensional region of linear extent  $L$ . Furthermore, assume that the single step distribution for a vectorial displacement  $\mathbf{x}$  of the random walk can be approximated by

$$p_{\Delta t}(\mathbf{x}) = (1 - Q)\delta(\mathbf{x}) + Q f_{\delta L}(\mathbf{x}). \quad (10)$$

Here  $\Delta t$  denotes the typical time between single steps,  $Q$  the fraction of walkers which jump a distance  $d > \delta L$  and  $(1 - Q)$  the fraction which remains in a disk defined by  $|\mathbf{x}| \leq \delta L$ . The function  $f_{\delta L}(\mathbf{x})$  comprises the power-law in the single steps, characteristic for Lévy flights:

$$f_{\delta L}(\mathbf{x}) = C \delta L^\beta |\mathbf{x}|^{-(2+\beta)} \quad |\mathbf{x}| \geq \delta L. \quad (11)$$

Inserting this into Eq. (10) one obtains that  $f_{\delta L}(\mathbf{x})$  is normalized to unity and that the normalization constant  $C$  is independent of the microscopic length  $\delta L$ . The Fourier-transform of  $p(\mathbf{x})$  is given by  $\tilde{p}(\mathbf{k}) = (1 - Q) + Q \tilde{f}_{\delta L}(\mathbf{k})$ . The Fourier-transform of the probability density function  $W_N(\mathbf{x})$  of the walker being located at a position  $\mathbf{x}$  after  $N$  steps can be computed in terms of  $\tilde{p}(\mathbf{k})$  according to

$$\tilde{W}_N(\mathbf{k}) = \tilde{p}(\mathbf{k})^N \approx (1 - Q \delta L^\beta |\mathbf{k}|^\beta)^N \approx e^{-QN |\delta L \mathbf{k}|^\beta}. \quad (12)$$

The relaxation time in a confined region is provided by the lowest mode  $k_{\text{min}} = L/2\pi$ . Inserted into (12) with  $N = t/\Delta t$  one obtains

$$T_{\text{eq}} \approx \delta T/Q (L/2\pi \delta L)^\beta = 68 \text{ days}. \quad (13)$$

Thus, after 2–3 months bank notes should have reached the equilibrium distribution. Surprisingly, the long time dispersal data does not reflect a relaxation within this time.

Fig. 6 shows secondary reports of bank notes with initial entry at Omaha, NE which have dispersed for times  $T > 100$  days (with an average time  $\langle T \rangle = 289$  days). Only 23.6% of the bank notes traveled farther than 800 km, the majority of 57.3% travelled an intermediate distance  $50 < r < 800$  km and a relatively large fraction of 19.1% remained within a radius of 50 km even after an average time of nearly one year. From Eq. (13) a much higher fraction of bills is expected to reach the metropolitan areas of the West Coast and the New England states after this time. This indicates that the simple Lévy flight picture for dispersal is incomplete. What causes this attenuation of the dispersal?

## 7 Scaling analysis

In order to understand the underlying cause of attenuated dispersal a useful theoretical tool is a spatiotemporal scaling analysis. The ordinary Lévy flight picture suggests that the process of money dispersal obeys a scaling relation  $\mathbf{X}(t) \sim t^{1/\beta}$  with an exponent  $\beta \approx 0.6$ . According to the empirical evidence of Fig. 6 the process is slowed down. Thus, a valid question would be: does the dispersal exhibit a scaling relation

$$\mathbf{X}(t) \sim t^{1/\mu} \quad (14)$$

with a somewhat larger exponent  $\mu > \beta$ ? If so, in what time window can one observe such a scaling and what is the exponent? Various methods for detecting a spatiotemporal scaling exist. One method is this: For a potential candidate of an exponent  $\mu$  one computes the distances divided by time of flights traveled raised to the power of  $1/\mu$ , i.e. the quantity

$$Z(t) = \frac{|\mathbf{X}(t)|}{t^{1/\mu}}. \quad (15)$$

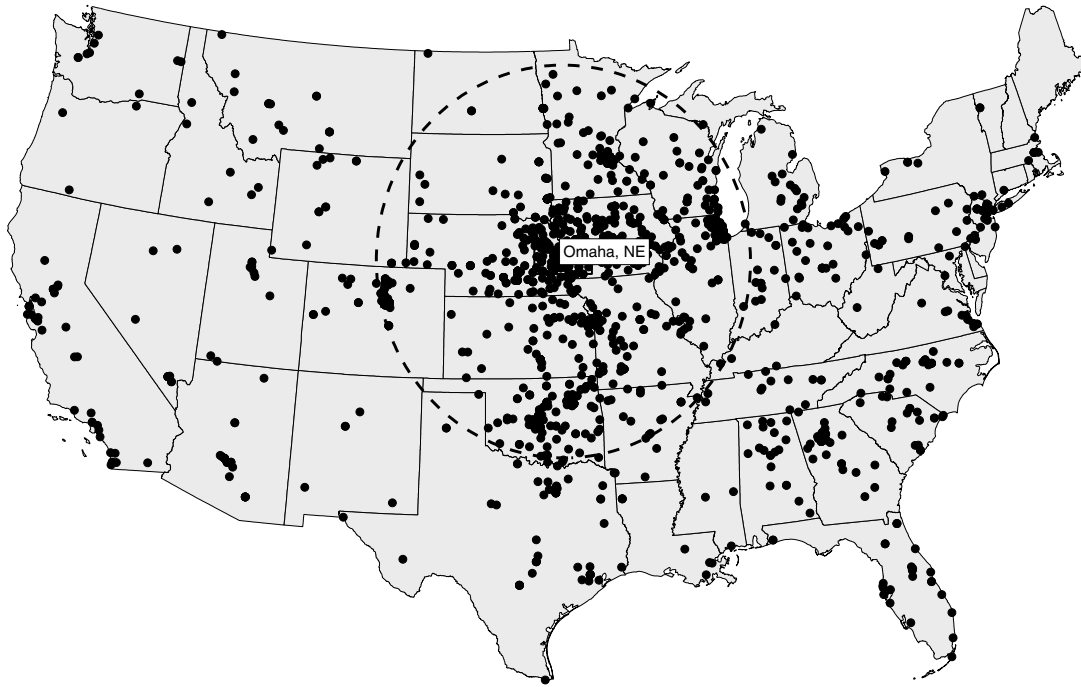


**Fig. 6.** Long time dispersal of bank notes with an initial entry in Omaha, NE. Points denote the location of the second report. Each bill travelled for a time greater than 100 days, with an average of 289 days. The dashed circle indicates the distance of 800 km from Omaha.

The scalar  $Z(t)$  is a stochastic time dependent quantity and in general with a time-dependent associated pdf  $p(z, t)$ . If the process  $\mathbf{X}(t)$  is scaling and for the right choice of exponent  $\mu$ ,  $p(z, t)$  is time-independent

$$p(z, t) = p(z). \quad (16)$$

As the pdfs  $p(\mathbf{x}, t)$  and  $p(z, t)$  of the processes  $\mathbf{X}(t)$  and  $Z(t)$ , respectively, are related by

$$p(z, t) = \left\langle \delta \left( z - |\mathbf{X}(t)|/t^{1/\mu} \right) \right\rangle \quad (17)$$

one can deduce that  $p(\mathbf{x}, t)$  must fulfill

$$p(\mathbf{x}, t) = t^{-D/\mu} f_{\mathbf{x}} \left( \mathbf{x}/t^{1/\mu} \right), \quad (18)$$

where the function  $f_{\mathbf{x}}$  is a scaling function. Likewise one obtains for the pdf  $p(r, t)$  of the distance  $R = |\mathbf{X}|$  traveled the relation

$$p(r, t) = t^{-1/\mu} f_r \left( r/t^{1/\mu} \right). \quad (19)$$

The quantity on the left-hand-side can be estimated from the data. Multiplied by the temporal factor on the right one obtains a quantity that depends on the ratio  $r/t^{1/\mu}$  only. The results of the scaling analysis of the money dispersal data is depicted in Fig. 7. For an exponent

$$\mu \approx 1$$

and in a time window of  $50 < T < 365$  days one finds that the data collapses on one curve which reflects the empirical scaling function  $f_r$ . Consequently, in a time-window of approx two months up to a year, money dispersal exhibits spatiotemporal scaling. Furthermore, the

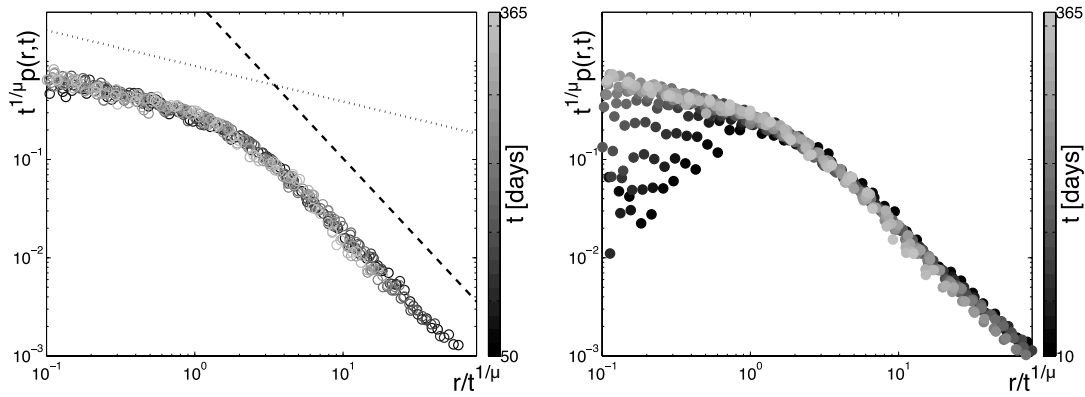


**Fig. 7.** Scaling analysis of money dispersal. Left: for times in the range of 50 to 365 days (indicated by the shade of grey) the quantity  $t^{1/\mu} p(r, t)$  is plotted against the ratio  $r/t^{1/\mu}$  for a scaling exponent  $\mu \approx 1$ . As all data point collapse on a single curve, the underlying process  $\mathbf{X}(t)$  exhibits spatiotemporal scaling. The emergent function  $f_r$  is the empirical scaling function of Eq. (19). Notice two regimes with power-law behavior. Right: deviation (dark grey) from the scaling function are observed, if short times are included ( $10 < t < 50$ ), consistent with the short time dispersal kernel of Fig. 5.

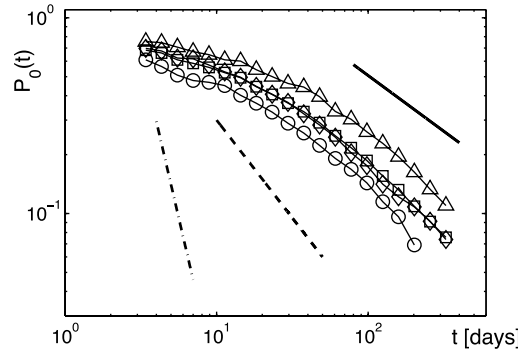


**Fig. 8.** The relative proportion  $P_0(t)$  of secondary reports within a short radius ( $r_0 = 20$  km) of the initial entry location as a function of time. Squares depict  $P_0(t)$  averaged over 25,375 initial entry locations. Triangles, diamonds, and circles show  $P_0(t)$  for the same classes as in Fig. 5. All curves decrease asymptotically as  $t^{-\xi}$  with an exponent  $\xi = 0.6 \pm 0.03$  indicated by the solid line. Ordinary diffusion in two dimensions predicts an exponent  $\xi = 1$  (black dashed line). Lévy flight dispersal with an exponent  $\beta = 0.6$  as suggested by the short time dispersal kernel (Fig. 5) predicts an even steeper decrease,  $\xi = 3.33$  (dot-dashed line).

empirical exponent  $\mu$  is greater than the exponent  $\beta$  promoted by the short time dispersal kernel

$$1 \approx \mu > \beta \approx 0.6,$$

reflecting the qualitative observation that the process is slowed down. Interestingly, the process is still superdiffusive, as  $\mu < 2$ . What could be a possible reason for this attenuation?

## 8 Scale free waiting times

A possible, conceptually straightforward explanations of this effect is a strong impact of the spatial inhomogeneity of the system. For instance, the typical time of rest in a geographical region might depend on local properties such as the population density. People might be less likely to leave large cities than e.g. suburban areas.

In order to address this issue one can investigated the relative proportion  $P_0^i(t)$  of bank notes which are reported again in a small (20 km) radius of the initial entry location  $i$  as a

function of time (Fig. 8). The quantity  $P_0^i(t)$  is a local quantity, it estimates the probability for a bank note of being reported at the initial location at time  $t$  a second time. In order to obtain reliable estimates this quantity is averaged over the above classes of initial entry locations (e.g. metropolitan areas, cities of intermediate size and small towns): For all classes one finds the asymptotic behaviour  $P_0(t) \sim A t^{-\eta}$  with an exponent  $\eta \approx 0.60 \pm 0.03$  and a coefficient  $A$ . The observed difference in values of the coefficient  $A$  reflect the impact of the spatial inhomogeneity of the system, i.e. bank notes are more likely to remain in highly populated areas. The exponent  $\eta$ , however, is approximately the same for all classes which indicates that waiting time and dispersal characteristics are universal and do not depend significantly on external factors such as the population density. Notice that for a pure two dimensional Lévy flight with index  $\beta$  the function  $P_0(t)$  scales as  $t^{-\eta}$  with  $\eta = 2/\beta$ . For  $\beta \approx 0.6$  (as put forth by Fig. 5) this implies  $\eta \approx 3.33$  [19], i.e. a five fold steeper decrease than observed, which clearly shows that dispersal cannot be described by a pure Lévy flight model. The measured decay is even slower than the decay exhibited by ordinary two-dimensional diffusion ( $\eta = 1$  [19]). This is very puzzling.

One way of slowing down dispersal are long periods of rest. In as much as an algebraic tail in the spatial displacements yields superdiffusive behavior, a tail in the probability density  $\psi(\Delta t)$  for times  $\Delta t$  between successive spatial displacements of an ordinary random walk can lead to subdiffusion. For instance, if  $\psi(\Delta t) \sim \Delta t^{-(1+\alpha)}$  with  $\alpha < 1$ , the position of an ordinary random walker scales according to  $X(t) \sim t^{2/\alpha}$  [14]. In combination with a power-law in the spatial displacements this ambivalence yields a competition between long jumps and long rests and can be responsible for the attenuation of dispersal [33].

## 9 Ambivalent processes

The idea of an antagonistic interplay between scale free displacements and waiting times can be explored within the framework of continuous time random walk (CTRW) introduced by Montroll and Weiss [34]. A CTRW consists of a succession of random displacements  $\Delta \mathbf{x}_n$  and random waiting times  $\Delta t_n$  each of which is drawn from a corresponding probability density function  $p(\Delta \mathbf{x})$  and  $\psi(\Delta t)$ . Spatial and temporal increments are assumed to be statistically independent. Furthermore, we assume that the spatial distribution is symmetric, i.e.  $p(\Delta \mathbf{x}) = p(|\Delta \mathbf{x}|)$ , and since the temporal increments are all positive  $\psi(\Delta t)$  is single sided. After  $N$  iterations the position of the walker and the elapsed time is given by

$$\mathbf{X}_N = \sum_n \Delta \mathbf{x}_n \quad \text{and} \quad T_N = \sum_n \Delta t_n,$$

respectively.

### 9.1 Scaling relation

These two equations relate position and time to step number. However, one is interested in the functional relationship of position and time. For instance, if the pdfs  $p(\Delta \mathbf{x})$  and  $\psi(\Delta t)$  possess a steep enough decrease for large arguments, i.e. existing moments, the central limit theorem implies that position scales with step number according to

$$\mathbf{X}_N \sim N^{1/2},$$

and time increases linearly with step number:

$$T_N \sim N.$$

Combining both scaling relationships one finds that in this case the process  $\mathbf{X}(t)$  exhibits ordinary diffusive scaling

$$\mathbf{X}(t) \sim t^{1/2}. \quad (20)$$

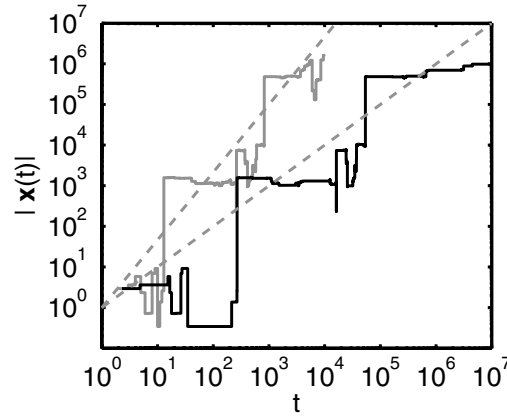


**Fig. 9.** Dispersal characteristics of an ordinary Lévy (grey) flight in comparison to an ambivalent process (black). The distance  $|\mathbf{X}(t)|$  from the origin as a function of time is depicted. The choice of exponents is  $\beta = 0.6$  for the Lévy process and  $\alpha = \beta = 0.6$  for the ambivalent process. The dashed lines indicate the heuristic scaling relations  $|\mathbf{X}(t)| = t^{1/\beta}$  and  $|\mathbf{X}(t)| = t^{\alpha/\beta}$ , respectively.

If, however both, spatial increments and waiting time possess an algebraic tail asymptotically, i.e.

$$p(\Delta\mathbf{x}) \sim \frac{1}{|\Delta\mathbf{x}|^{2+\beta}} \quad \text{and} \quad \psi(\Delta t) \sim \frac{1}{\Delta t^{1+\alpha}}, \quad (21)$$

with spatial and temporal exponents  $0 < \beta < 2$  and  $0 < \alpha < 1$ , respectively, the second moment of  $\Delta\mathbf{x}$  as well as the first moment of  $\Delta t$  are divergent. This implies a scaling of position of the form

$$\mathbf{X}_N \sim N^{1/\beta}, \quad (22)$$

as observed for ordinary Lévy flights but a superlinear scaling of time with step number as well:

$$T_N \sim N^{1/\alpha}. \quad (23)$$

The combination of these two scaling relation give a heuristic scaling of position with time which depends on the ratio of both exponents  $\alpha$  and  $\beta$

$$\mathbf{X}(t) \sim t^{\alpha/\beta}. \quad (24)$$

Comparing with the scaling relation of superdiffusive ordinary Lévy processes,  $\mathbf{X}(t) \sim t^{1/\beta}$ , Eq. (37) one sees that long waiting times slow down the process as the temporal exponent is less than unity. This is easily demonstrated by a numerical realization of an ambivalent process as depicted in Fig. 9. Clearly long waiting times slow down the process and the scaling relation (24) is valid.

The scaling relation (24) implies that by choosing waiting time and jump length exponents in their valid ranges one can generate processes with any type of spatiotemporal scaling. The phase diagram (Fig. 10) illustrates the various processes one can generate by varying the exponents  $\alpha$  and  $\beta$  and show the limiting processes. For instance when  $2\alpha > \beta$  the process is superdiffusive and when  $2\alpha < \beta$  the process is subdiffusive. The limiting processes of ordinary Lévy flights, fractional Brownian motion (regular subdiffusion) and ordinary diffusion are attained by choosing  $(\alpha = 1, 0 < \beta < 2)$ ,  $(0 < \alpha < 1, \beta = 2)$  and  $(\alpha = 1, \beta = 2)$ , respectively. Note that the family of processes for which the ratio of exponents is  $\alpha/\beta = \text{const.}$  exhibit the same spatiotemporal scaling. This does not imply however, that these processes are identical and will become clear below. This is best illustrated for a choice of processes which fulfill  $2\alpha = \beta$ . These exhibit ordinary diffusive scaling but nevertheless are not diffusion processes.

In Fig. 11 such a quasi-diffusive process is compared with an ordinary diffusion process. This example illustrates that processes with identical ratio  $\alpha/\beta$  are geometrically quite different

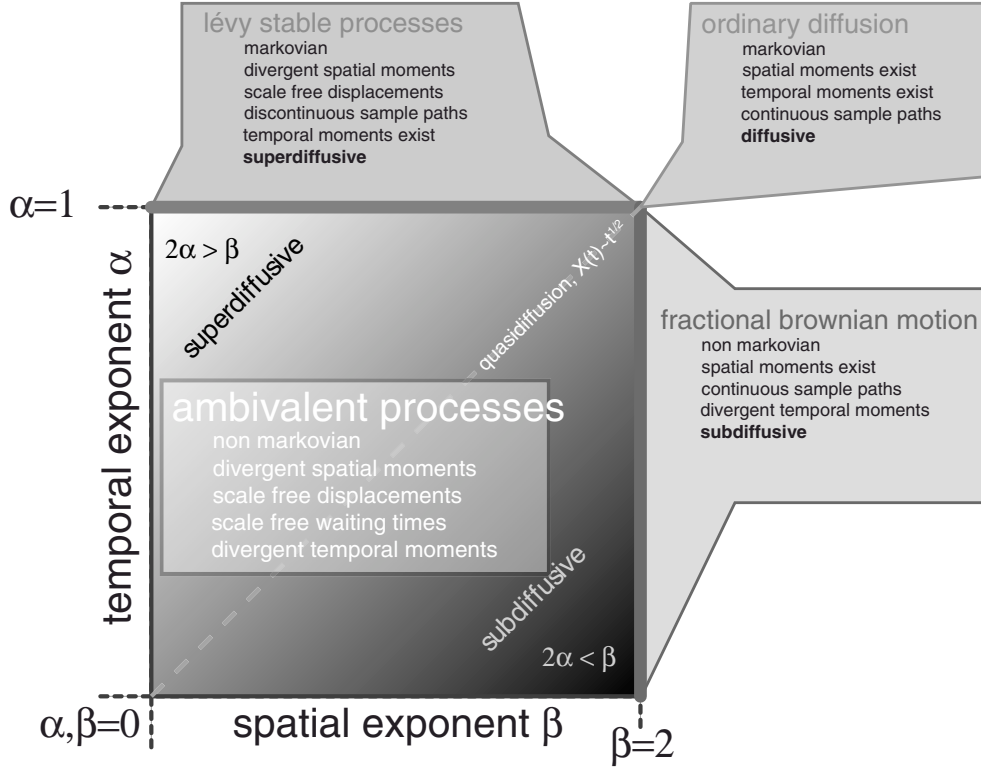


**Fig. 10.** Phase diagram for ambivalent anomalous diffusion processes with scale-free waiting times and scale-free spatial displacements and their limiting processes. The valid ranges for temporal and spatial exponents  $\alpha$  and  $\beta$  are  $(0, 1]$  and  $(0, 2]$ , respectively.

but also that in order to fully comprehend the properties of ambivalent anomalous diffusion processes one is required to compute the pdf  $W(\mathbf{x}, t)$  for the process  $\mathbf{X}(t)$  or a dynamical equation for it.

## 9.2 The limiting function for ambivalent processes

The quantity of interest is the position  $\mathbf{X}(t)$  after time  $t$ . The probability density  $W(\mathbf{x}, t)$  for this process can be computed in a straightforward fashion [14] and can be expressed in terms of the spatial distribution  $p(\Delta\mathbf{x})$  and the temporal distribution  $\psi(\Delta t)$ . The Fourier-Laplace transform of  $W(\mathbf{x}, t)$  is given by

$$\tilde{W}(\mathbf{k}, u) = \frac{1 - \tilde{\psi}(u)}{u \left( 1 - \tilde{\psi}(u) \tilde{p}(\mathbf{k}) \right)}, \quad (25)$$

which can be computed within the CTRW framework, for details see [14, 35]. In Eq. (25)  $\tilde{\psi}(u)$  and  $\tilde{p}(\mathbf{k})$  denote the Laplace- and Fourier transform of  $\psi(\Delta t)$  and  $p(\Delta\mathbf{x})$ , respectively. The probability density  $W(\mathbf{x}, t)$  is then obtained by inverse Laplace-Fourier transform

$$W(\mathbf{x}, t) = \frac{1}{(2\pi)^3 i} \int_{c-i\infty}^{c+i\infty} du \int d\mathbf{k} e^{ut - i\mathbf{k}\mathbf{x}} \tilde{W}(\mathbf{k}, u). \quad (26)$$

When both, the variance of the spatial steps  $\langle (\Delta\mathbf{x})^2 \rangle = \sigma^2$  and the expectation value  $\langle \Delta t \rangle = \tau$  of the temporal increments exist the Fourier- and Laplace transform of  $p(\Delta\mathbf{x})$  and  $\psi(\Delta t)$  are

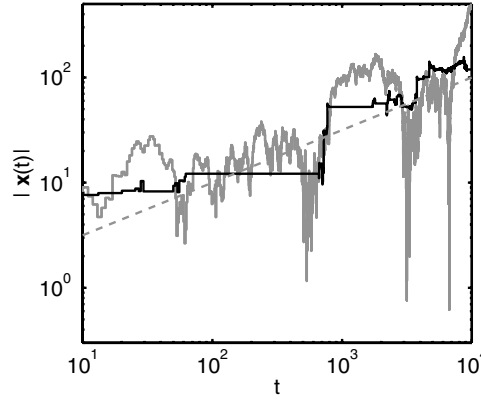


**Fig. 11.** Two processes that exhibit diffusive scaling, i.e.  $|\mathbf{X}(t)| \sim t^{1/2}$  (dashed line). The grey process is ordinary diffusion, the black one an ambivalent anomalous diffusion process with exponents  $\alpha = 3/4$  and  $\beta = 3/2$  which implies diffusive scaling. Note that the geometry of both processes are remarkably different.

given by

$$\tilde{p}(\mathbf{k}) = 1 - \sigma^2 \mathbf{k}^2 + \mathcal{O}(\mathbf{k}^4) \quad (27)$$

$$\tilde{\psi}(u) = 1 - \tau u + \mathcal{O}(u^2), \quad (28)$$

for small arguments, which yield the asymptotics of the process. Inserted into Eq. (25) and employing inversion (26) one obtains

$$W(\mathbf{x}, t) = (2\pi Dt)^{-1} e^{-\mathbf{x}^2/2Dt} \quad (29)$$

in this limit with  $D = \sigma^2/\tau$ . Thus, whenever  $\langle(\Delta\mathbf{x})^2\rangle$  and  $\langle\Delta t\rangle$  are finite a CTRW is asymptotically equivalent to ordinary Brownian motion as expected.

The situation is drastically different, when both,  $p(\Delta\mathbf{x})$  and  $\psi(\Delta t)$  exhibit algebraic tails of the form

$$p(\Delta\mathbf{x}) \sim \frac{1}{|\Delta\mathbf{x}|^{2+\beta}} \quad 0 < \beta < 2 \quad \text{and} \quad \psi(\Delta t) \sim \frac{1}{\Delta t^{1+\alpha}} \quad 0 < \alpha < 1. \quad (30)$$

In this case one obtains for the asymptotics of  $\tilde{p}(\mathbf{k})$  and  $\tilde{\psi}(u)$ :

$$\tilde{p}(\mathbf{k}) = 1 - D_\beta |\mathbf{k}|^\beta + \mathcal{O}(k^2) \quad (31)$$

$$\tilde{\psi}(u) = 1 - D_\alpha u^\alpha + \mathcal{O}(u). \quad (32)$$

Inserted into (25) yields the solution for the process in Fourier-Laplace space:

$$\tilde{W}_{\alpha,\beta}(\mathbf{k}, u) = \frac{u^{-1}}{1 + D_{\alpha,\beta} |\mathbf{k}|^\beta / u^\alpha}, \quad (33)$$

where the constant  $D_{\alpha,\beta} = D_\beta/D_\alpha$  is a generalized diffusion coefficient. After inverse Laplace transform the solution in  $(\mathbf{x}, t)$  coordinates reads:

$$W(\mathbf{x}, t) = \frac{1}{2\pi} \int d\mathbf{k} e^{-i\mathbf{k}\mathbf{x}} E_\alpha(-D_{\alpha,\beta} |\mathbf{k}|^\beta t^\alpha). \quad (34)$$

Here,  $E_\alpha$  is the Mittag-Leffler function defined by

$$E_\alpha(z) = \sum_{n=0}^{\infty} \frac{z^n}{\Gamma(1 + \alpha n)}. \quad (35)$$

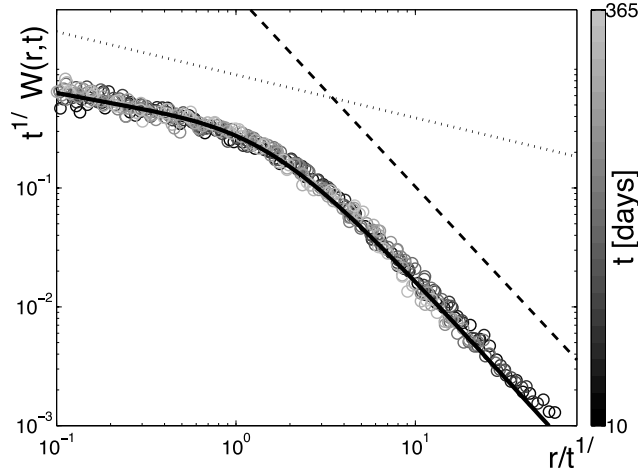


**Fig. 12.** The empirical radial probability density function  $W_r(r, t)$  and theoretical scaling function  $\tilde{L}_{\alpha, \beta}$ . In order to extract scaling the function  $W(r, t)$  is shown for various but fixed values of time  $t$  between 10 and 365 days as a function of  $r/t^{1/\mu}$ . For  $\mu \approx 1.0$  the measured (circles) curves collapse on a single curve and the process exhibits universal scaling. The scaling curve represents the empirical limiting density  $F$  of the process. The asymptotic behaviour for small (dotted line) and large (dashed line) arguments  $y = r/t^{1/\mu}$  is given by  $y^{-(1-\xi_1)}$  and  $y^{-(1+\xi_2)}$ , respectively, with estimated exponents  $\xi_1 = 0.63 \pm 0.04$  and  $\xi_2 = 0.62 \pm 0.02$ . According to our model these exponents must fulfill  $\xi_1 = \xi_2 = \beta$  where  $\beta$  is the exponent of the asymptotic short time dispersal kernel (Fig. 5), i.e.  $\beta \approx 0.6$ . The superimposed solid line represents the scaling function predicted by our theory with spatial and temporal exponents  $\beta = 0.6$  and  $\alpha = 0.6$ .

which is a generalization of the exponential function to which it is identical for  $\alpha = 1$ . The integrand  $E_\alpha(-D_{\alpha, \beta} |\mathbf{k}|^\beta t^\alpha)$  is the characteristic function of the process. As it is a function of  $\mathbf{k}t^{\alpha/\beta}$ , the probability density  $W(\mathbf{x}, t)$  can be expressed as

$$W(\mathbf{x}, t) = t^{-2\alpha/\beta} L_{\alpha, \beta}(\mathbf{x}/t^{\alpha/\beta}) \quad (36)$$

in which the function  $L_{\alpha, \beta}(\mathbf{z}) = (2\pi)^{-1} \int d\mathbf{k} E_\alpha(-|\mathbf{k}|^\beta - i\mathbf{k}\mathbf{z})$  is a universal scaling function which is characteristic for the process and depends on the two exponents  $\alpha$  and  $\beta$  only. Most importantly, one can extract the spatio-temporal scaling of the ambivalent process from (34)

$$\mathbf{X}(t) \sim t^{\alpha/\beta}, \quad (37)$$

identical to the relation derived heuristically above. The ratio of the exponents  $\alpha/\beta$  resembles the interplay between sub- and superdiffusion. For  $\beta = 2\alpha$  the process exhibits the same scaling as ordinary Brownian motion, despite the crucial difference of infinite moments and a non-Gaussian shape of the probability density  $W(\mathbf{x}, t)$ . The function  $W(\mathbf{x}, t)$  is a probability density for the vectorial displacements  $\mathbf{x}$ . From Eqs. (34) and (36) we can compute the probability density  $W_r(r, t)$  for having traveled the scalar distance  $r = |\mathbf{x}|$  by integration over all angles:

$$W_r(r, t) = t^{-\alpha/\beta} \tilde{L}_{\alpha, \beta}(r/t^{\alpha/\beta}), \quad (38)$$

with a universal scaling function  $\tilde{L}_{\alpha, \beta}$  which can be expressed in terms of  $L_{\alpha, \beta}$ .

Finally, the validity of the ambivalent CTRW model can be tested against the dollar bill dispersal data by estimating the empirical  $W_r(r, t)$  from the entire dataset of a little over half a million displacements and elapse times and compared to Eq. (38). The results of this analysis are compiled in Fig. 12. Comparing with the spatio-temporal scaling promoted by the CTRW model  $r(t) \sim t^{\alpha/\beta}$  a value of  $\mu = 1$  would imply that temporal and spatial exponents are the same

$$\alpha = \beta. \quad (39)$$

Combined with the results obtained from the short time analysis yields

$$\alpha = \beta = 0.6. \quad (40)$$

A final test of the CTRW model is the comparison of the empirically observed scaling function  $F$  with the predicted scaling function  $\tilde{L}_{\alpha,\beta}$  for the values of the exponents in Eq. (40). As depicted in Fig. 12 the asymptotics of the empirical curve is given by  $y^{-(1-\xi_1)}$  and  $y^{-(1+\xi_2)}$  for small and large arguments  $y = r/t^{1/\mu}$ , respectively. Both exponents fulfill  $\xi_1 \approx \xi_2 \approx 0.6$ . By series expansions one can compute the asymptotics of the CTRW scaling function  $\tilde{L}_{\alpha,\beta}(y)$  which gives  $y^{-(1-\beta)}$  and  $y^{-(1+\beta)}$  for small and large arguments, respectively. Consequently, as  $\beta \approx 0.6$  the theory agrees well with the observed exponents. For the entire range of  $y$  one can compute  $L_{\alpha,\beta}(y)$  by numeric integration for  $\beta = \alpha = 0.6$  and superimpose the theoretical curve on the empirical one. The agreement is very good and supports the CTRW model. In summary, this is solid evidence that the dispersal of bank notes can be accounted for by a simple random walk process with scale free jumps and scale free waiting times.

The question remains how the dispersal characteristics of bank notes carries over to the dispersal of humans and more importantly to the spread of human transmitted diseases. In this context one can safely assume that the power law with exponent  $\beta = 0.6$  of the short time dispersal kernel for bank notes reflects the human dispersal kernel as only short times are considered. However, as opposed to bank notes humans tend to return from distant places they travelled to. This however, has no impact on the dispersal of pathogens which, much like bank notes, are passed from person to person and have no tendency to return.

The issue of long waiting times is more subtle. One might speculate that the observed algebraic tail in waiting times of bank notes is a property of bank note dispersal alone. Long waiting times may be caused by bank notes which exit the money tracking system for a long time, for instance in banks. However, if this were the case the inter-report time statistics would exhibit a fat tail. Analysing the interreport time distribution one finds an exponential decay which suggests that bank notes are passed from person to person at a constant rate. Furthermore, if one assumes that humans exit small areas at a constant rate which is equivalent to exponentially distributed waiting times and that bank notes pass from person to person at a constant rate, the distribution of bank note waiting times would also be exponential in contrast to the observed power law.

Based on this analysis one can conclude that the dispersal of bank notes and human transmitted diseases can be accounted for by a continuous time random walk process incorporating scale free jumps as well as long waiting time in between displacements.

However, a word of caution is necessary at this point. The above model for the dispersal of bank notes is only an initial step towards a better understanding of human mobility and universal features of human transportation networks on global scales. One obvious reason is that the CTRW model, despite its wonderful agreement with the data, is a heuristic model and represents a population averaged model. As alluded to above, spatial heterogeneities do impact on the dispersal characteristics quantitatively although they do not change the qualitative features of the dispersal process. This is analogous to a situation in which a Brownian particle diffuses on a two-dimensional liquid layer which in turn is heterogeneously heated from below. A position dependent temperature profile would introduce a position dependent diffusion coefficient for the particle which changes the local diffusion properties. Despite the fact that such a particle performs ordinary diffusion at every location one would have to incorporate a the position dependent diffusion coefficient in a quantitative description of the particle's motion in the corresponding Fokker-Planck equation. Replacing the position dependent diffusion coefficient by a spatially averaged quantity only gives an incomplete description of the system. A promising line of investigation could then be provided by the concept of superstatistics introduced by Beck and Cohen [36] that is introduced and explained in detail in Chapter (??) in this book.

In the context of human travel behavior, one would have to determine position dependencies in the generalized diffusion coefficient for which the originally explored wheresgeorge dataset is insufficient. Alternatively, one could investigate these processes within the framework of complex embedded networks in which places in the United States are nodes of the network and the flux of bills weighted, non-negative links between them. This approach introduces a number

of powerful analytic and numeric techniques which in my view could complete our understanding of human travel in our globalized world.

## References

1. J.M. Bullock, R.E. Kenward, R.S. Hails (eds.), *Dispersal Ecology* (Blackwell, Malden, Massachusetts, 2002)
2. J.D. Murray, *Mathematical Biology* (Springer-Verlag, Berlin, Heidelberg, New York, 1993)
3. J. Clobert, *Dispersal* (Oxford Univ. Press, Oxford, 2001)
4. K. Nicholson, R.G. Webster, *Textbook of Influenza* (Blackwell Publishing, Malden, MA, USA, 1998)
5. B.T. Grenfell, O.N. Bjornstad, J. Kappey, *Nature* **414**, 716 (2001)
6. M.J. Keeling, M.E.J. Woolhouse, D.J. Shaw, L. Matthews, M. Chase-Topping, D.T. Haydon, S.J. Cornell, J. Kappey, J. Wilesmith, B.T. Grenfell, *Science* **294**, 813 (2001)
7. L. Hufnagel, D. Brockmann, T. Geisel, *Proc. Natl. Acad. Sci. USA* **101**, 15124 (2004)
8. N.C. Grassly, C. Fraser, G.P. Garnett, *Nature* **433**, 417 (2005)
9. R.J. Webby, R.G. Webster, *Science* **302**, 1519 (2003)
10. D. Brockmann, L. Hufnagel, T. Geisel *SARS: A Case Study in Emerging Infections*, edited by A. McLean, R. May, J. Pattison, R. Weiss (Oxford University Press, Oxford, 2005), p. 81
11. R.M. Anderson, R.M. May, B. Anderson, *Infectious Diseases of Humans: Dynamics and Control* (Oxford Univ. Press, USA, 1992)
12. D. Brockmann, L. Hufnagel, T. Geisel, *Nature* **439**, 462 (2006)
13. M.F. Shlesinger, *Lvy Flights and Related Topics in Physics* (Springer Verlag, Berlin, 1995)
14. R. Metzler, J. Klafter, *Phys. Rep.-Rev. Sect. Phys. Lett.* **339**, 1 (2000)
15. M. Kot, M.A. Lewis, P. vandenDriessche, *Ecology* **77**, 2027 (1996)
16. C.W. Gardiner, *Handbook of Stochastic Methods* (Springer Verlag, Berlin, 1985)
17. W. Feller, *An Introduction to Probability Theory and Its Application*, Vol. I (Wiley, New York, 1968)
18. R.A. Fisher, *Ann. Eugen.* (1937)
19. W. Feller, *An Introduction to Probability Theory and Its Application*, Vol. 2 (Wiley, New York, 1971)
20. R. Nathan, G.G. Katul, H.S. Horn, S.M. Thomas, R. Oren, R. Avissar, S.W. Pacala, S.A. Levin *Nature* **418**, 409 (2002)
21. M. Schoeder, *Fractals, Chaos, Power Laws. Minutes from an Infinite Paradise* (W.H. Freeman and Company, New York, 1991)
22. G.M. Viswanathan, S.V. Buldyrev, S. Havlin, M.G.E. da Luz, E.P. Raposo, H.E. Stanley, *Nature* **401**, 911 (1999)
23. F. Bartumeus, F. Peters, S. Pueyo, C. Marrase, J. Catalan, *Proc. Natl. Acad. Sci. USA* **100**, 12771 (2003)
24. A. Marell, J.P. Ball, A. Hofgaard, *Canad. J. Zool.-Rev. Canad. Zool.* **80**, 854 (2002)
25. G.M. Viswanathan, V. Afanasyev, S.V. Buldyrev, E.J. Murphy, P.A. Prince, H.E. Stanley, *Nature* **381**, 413 (1996)
26. G. Ramos-Fernandez, J.L. Mateos, O. Miramontes, G. Cocho, H. Larralde, B. Ayala-Orozco, *Behav. Ecol. Sociobiol.* **55**, 223 (2004)
27. R.P.D. Atkinson, C.J. Rhodes, D.W. Macdonald, R.M. Anderson, *Oikos* **98**, 134 (2002)
28. M.F. Shlesinger, G.M. Zaslavsky, U. Frisch (eds.), *Lévy flights and Related Topics in Physics* (Springer, Berlin, 1995)
29. D. Brockmann, T. Geisel, *Phys. Rev. Lett.* **90**, 170601 (2003)
30. D. Brockmann, I.M. Sokolov, *Chem. Phys.* **284**, 409 (2002)
31. T. Geisel, J. Nierwetberg, A. Zacherl, *Phys. Rev. Lett.* **54**, 616 (1985)
32. M.F. Shlesinger, *Nat. Phys.* **2**, 69 (2006)
33. M.F. Shlesinger, J. Klafter, Y.M. Wong, *J. Stat. Phys.* **27**, 499 (1982)
34. E.W. Montroll, G.H. Weiss, *J. Math. Phys.* **6**, 167 (1965)
35. A.I. Saichev, G.M. Zaslavsky, *Chaos* **7**, 753 (1997)
36. C. Beck, E.G.D. Cohen, *Phys. a-Stat. Mech. Appl.* **322**, 267 (2003)